Tooth contact analysis of spur gears. Part 1- SAM analysis of standard gears

Spiridon Creţu*, *Nicolae* Pop, and *Stelian* Cazan
Technical University of Iaşi, Mechanical Engineering Department, 63 D. Mangeron St., Iaşi, Romania

Abstract. The involute gears are sensitive to the misalignment of their axes which determines transmission errors and perturbations of pressures distributions along the tooth flank. The concentrated contacts in gears are no longer as Hertz type. A semi-analytical method was developed to find the contact area, pressures distribution and depth stresses state. The matrix of initial separations is found analytically for standard and non-standard spur gears. The presence of misalignment as well as the flank crowning and flank end relief are included in the numerical analysis process.

1 Introduction

Under real running condition the meshing is altered by various deviations of the machine parts involved [1], but also by elastic deformations [2], which determine transmission errors and perturbations of pressures distributions along the flank, especially at its end sides, Figure1a. The pressures concentrations accelerate the fatigue and wear phenomena resulting a much shorter life for the machine parts subjected to rolling contact [3]. The concentrated contacts in gears meshing are no longer of Hertz type [4-6], and no straight analytical solutions is available. Semi-analytical methods have been developed to find the contact area, pressures distribution and depth stresses state [7-9]. For spur and helical gears some techniques as flank crowning or flank relieving, Figure 1b, are commonly used to modify the initial line contact to a localized bearing contact [5, 6]. The normal load acts along the contact line and a common contact area develops. The shape and size of the common contact area, as well as the pressures distribution on this area, are unknown.

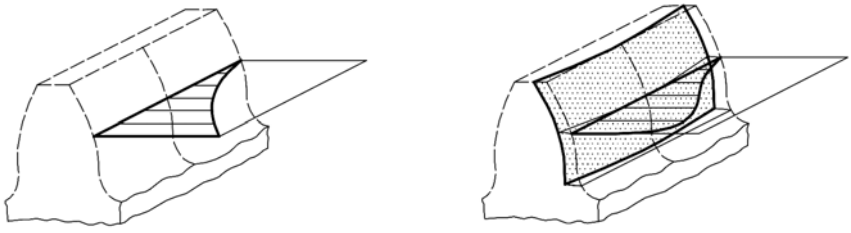

a b

Fig.1. The pressures concentration (a) and the effect of flank crowning (b).

* Corresponding author: spcretu@tuiasi.ro

2 SAM modelling of non-Hertz concentrated contacts

The semi-analytical method uses the initial (no load) separations between surfaces of the conjugate teeth that sustain the meshing process. A virtual rectangular contact area, denoted A_v, is built on the common tangent plane, around the initial contact point, and a Cartesian system *(x, y, z)* is introduced, the *x-O-y* plane being the common tangent plane, Figure 2.

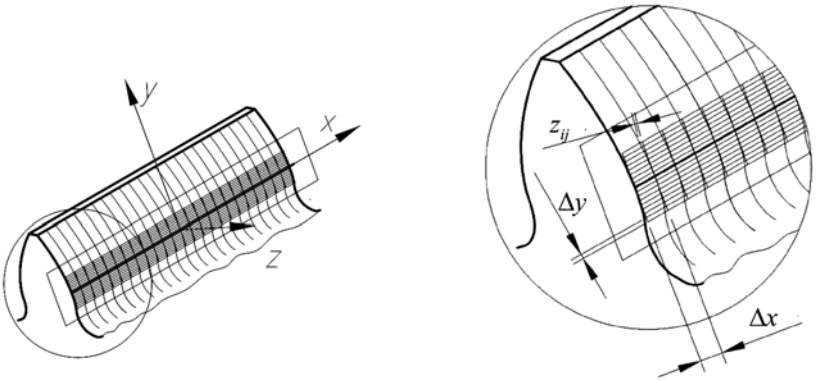

Fig. 2. The virtual rectangular contact area.

A uniformly spaced rectangular array is built on the virtual rectangular contact area with the grid sides parallel to the *x* and *y*-axes. The nodes of the grid are denoted by *(i, j)*, where indices *i* and *j* refer to the N_x grid columns and N_y grid rows, respectively. The real pressure distribution is approximated by a virtual pressure distribution, characterized by unknown constant values p_{ij} inside of each (i,j) patch [8, 9]. The surface deformation is modeled by the following six linear algebraic equations:

a) geometric equation of the elastic contact:

$$g_{ij} = h_{ij} + w_{ij} - \delta_0 \quad (1)$$

where: g_{ij} is the gap between the normal loaded surfaces, h_{ij} is the separation between unloaded surfaces, w_{ij} is the elastic deformation of the two surfaces, measured along the normal load, and δ_0 is the rigid displacement of the contacting bodies;

b) equation of the normal surface displacement:

$$w_{ij} = \sum_{k=0}^{Nx-1} \sum_{j=0}^{Ny-1} (K_{i-k,j-l} * p_{kl}) \quad (2)$$

c) load balance equation

$$\Delta x \Delta y \sum_{i=0}^{Nx-1} \sum_{j=0}^{Ny-1} p_{ij} = F \quad (3)$$

d) constraint equation of non-penetration:

$$g_{ij} = 0, \xrightarrow{yields} p_{ij} > 0, \ (i,j) \exists A_r \quad (4)$$

e) constraint equation of non-adhesion:

$$g_{ij} > 0, \xrightarrow{yields} p_{ij} = 0, \ (i,j) \notin A_r \quad (5)$$

f) *elastic-perfect plastic* behavior of the material:

$$p_{ij} \geq p_Y \Rightarrow p_{ij} = p_Y \quad (6)$$

where p_Y is the value of the pressure able to initiate the plastic yield.

The influence function K_{ij} represents the value of the surface deformation created in the point *(i, j)* by the unit pressure acting in the elementary rectangle *(k, l)* [9].

The components of the stress tensor are obtained by superposition

$$\sigma_{ij}(x,z,y,) = \sum_{k=0}^{Nx-1}\sum_{l=0}^{Ny-1}\left(C_{ijkl} * p_{kl}\right) \quad (7)$$

where the influence function $C_{ijkl}(x,y,z)$ describes the stress component $\sigma_{ij}(x,y,z)$ due to a unit pressure acting in the patch *(k, l)*, [10]. A single-loop conjugate gradient method was used to solve the mentioned algebraic system of equations. To increase the efficiency of the numerical algorithm, a dedicated discrete fast Fourier transform routine for 3D contact problems was used to solve the convolution products. The entire algorithm has been applied in a C++ computer code, named Non-Hertz [9, 10].

3 Matrix of separations

Spur involute gears are in line contact at every instant and consequently the virtual rectangular contact area is built having the contact line as median line. The half-width of the virtual rectangular area has a value b_v related to the value b_H obtained considering the Hertz hypothesis. The target is to determine the value h_{ij} of the initial separation in each mesh point *(i, j)* of the virtual rectangle. Two fixed coordinate systems, $O_1v_1w_1$ and $O_2v_2w_2$, are attached to pinion and gear Figure 3a, and two coordinates transformations are operated.

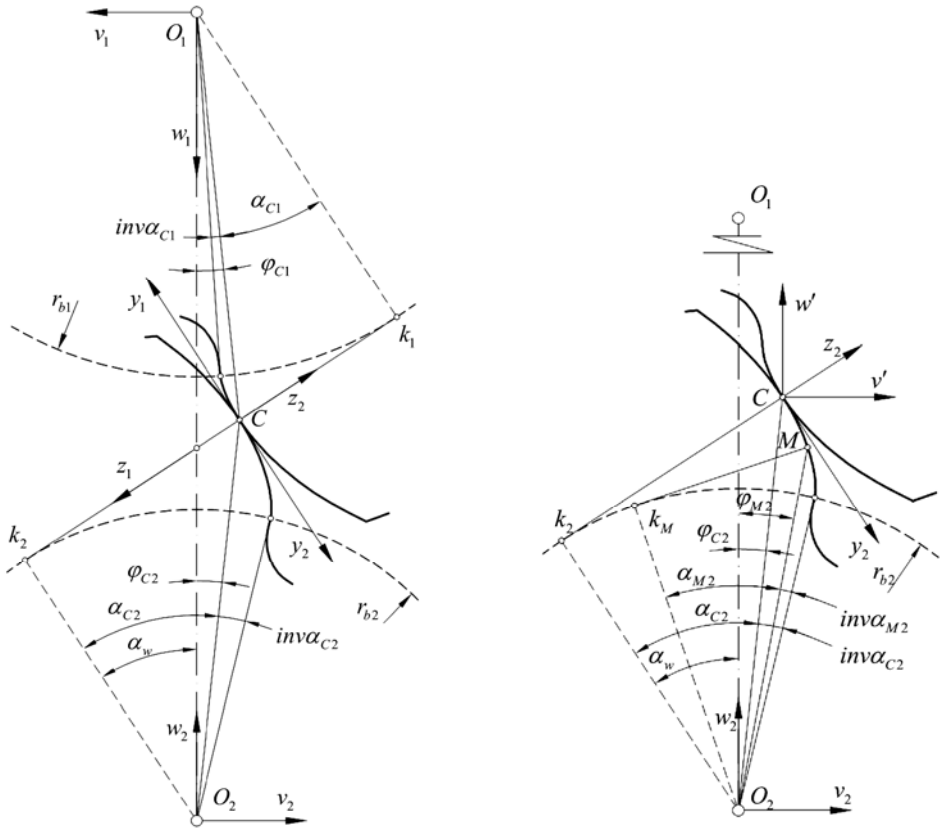

a b

Fig. 3. The main geometric elements and coordinate systems.

The first one is a translation from the fixed system $O_2v_2w_2$ to the mobile coordinate system $v'Cw'$, Figure 3b. The second coordinate transformation is a rotation with the angle θ, needed to obtain the *Cz* axis along the common normal of the teeth surfaces and *Cy* axis in the tangent plane of the contact point, Figure 3b. In the mesh grid of virtual rectangular area the point *(i,j)* is located at the distance y_j from the contact line. A mobile point *M,* with the position angle φ_{M2}, Figure 3b is considered on the flank of gear 2:

$$\varphi_{M2} = \varphi_{C2} - (\text{inv}\alpha_{M2} - \text{inv}\alpha_{C2}) \tag{8}$$

For gear 2 and point $M_2(x_i, y_j)$ the pressure angle α_{M2} is found as solution of the equation:

$$f(\alpha_{M2}) = y_{M2} - y_j = \frac{r_{b2}}{\cos\alpha_{M2}}\sin(\theta + \varphi_{M2}) - \frac{r_{b2}}{\cos\alpha_{C2}}\sin(\theta + \varphi_{C2}) - y_j = 0 \tag{9}$$

The Newton-Raphson iterative method provides the solution α_{M2}.

For point *(i,j)*, situated on virtual contact area, the equations (8, 9) give the value of initial separation $h2_{ij}$ between the tangent plane and flank surface of gear 2:

$$h2_{ij} = z_{M2[i,j]} \tag{10}$$

The same technique is used to obtain the initial separation $h1_{ij}$ [11]:

$$h1_{ij} = z_{M1[i,j]} \tag{11}$$

The normal separation between the surfaces of the meshing teeth is:

$$h_{ij} = h1_{ij} + h2_{ij} \tag{12}$$

The misalignment as well as the flank crowning or end flank relief are further included in the computing process for the matrix of initial separations data. The Non-Hertz software uses the separations matrix as initial data in an iterative process to obtain the pressures distribution, contact area and stresses states in the shallow layers of loaded teeth [9, 10].

4 TCA analysis of standard spur gears

The numerical analysis has been performed using the data for standard spur gears: $\alpha_0 = 20^0,\ h^*_{ao} = 1,\ c^*_0 = 0.25,\ \rho^*_0 = 0.38$ [11].
$z_1 = 25,\ z_2 = 51,\ m_n = 4$ mm, $x_1 = 0,\ x_2 = 0,\ B = 50$ mm.
The nominal power parameters were: $T_2 = 30$ kW, ϖ_2= 52.35 rad/s.

4.1 Standard spur gears - the edge effect

The phenomenon of pressures concentration at the end sides of the line contact with finite length is called *edge effect* [5, 13, 14]. To be in agreement with experimental evidence of the edge effect Guilbault [13] introduces a correction factor ψ into the 3D computational algorithm. In case of a flank with sharp edges the high values of pressures developed in the end areas of the flank might induce plastic deformations able to change locally the contact geometry and to attenuate the edge effect [14].To avoid the cumbersome calculations needed to evaluate the edge effect in standard spur gears, the present algorithm considers, for both sides of the flank, a chamfer with the radius R_{ch}=*0.2* mm.

4.2 Numerical analysis

Standard spur gears, having a straight line lead (SL-lead), obtained with good manufacturing practice and operating in ideal conditions, were first considered.

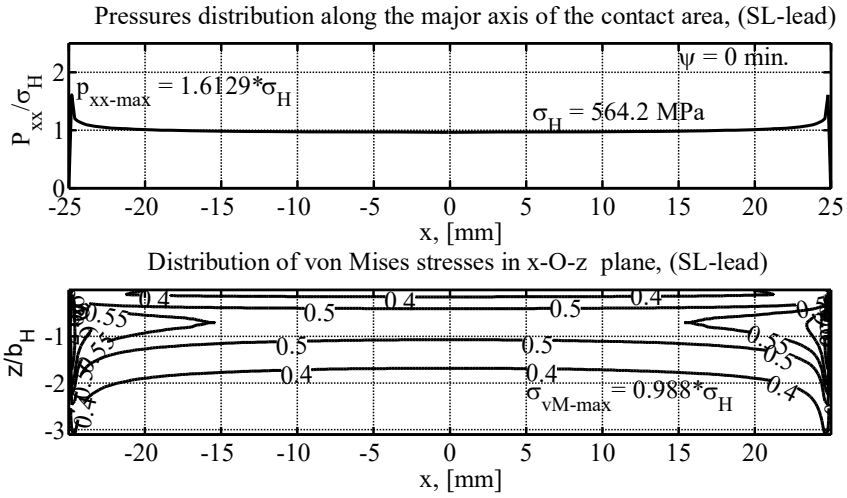

Fig. 4. Distributions of pressures and von Mises stresses for operating without misalignment.

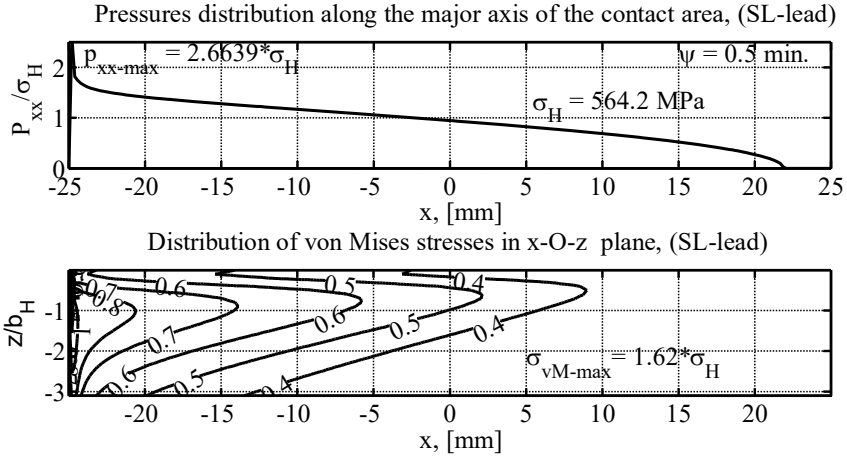

Fig. 5. Distributions of pressures and von Mises stresses for operating with misalignment, $\psi =$ 0.5 min.

The pressures distribution is presented in Figure 4 for the case when the contact point *C* is in the meshing pole, $\alpha_{C1} = \alpha_{C2} = \alpha_w = 20^o$. Along the tooth flank the maximum pressure is very close to the Hertz pressure except end sides areas where the edge effect manifests, Figure 4.

The edge effect becomes much damaging when even a small misalignment exists. Figure 5 depicts the pressures distribution obtained using the same operating data added with a misalignment of $\psi = 0.5$ min. As effect of this small misalignment, the p_{max}/σ_H ratio between the maximum value of pressure and Hertzian stress, increased from 1.61 to 2.66. Some of plasticity criteria consider the value of von Mises stress as responsible for starting the material yielding inside the stressed volume [9], and for the initiation of the rolling contact fatigue [3, 15]. In this respect the σ_{vM-max}/σ_H ratio between the maximum value of von Mises stress and Hertz stress, increased from 0.99 to 1.62.

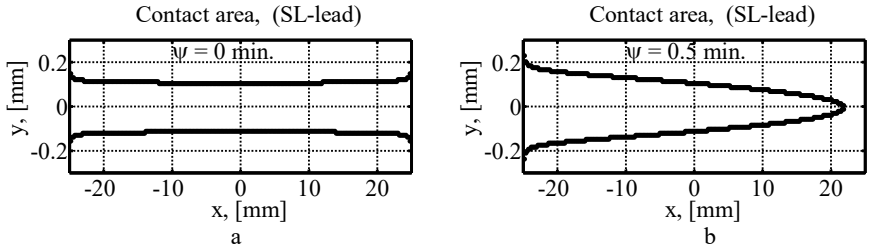

Fig. 6. Contact areas: a- operating in ideal conditions; b- operating with misalignment.

The shape and size of the contact area suffer major modifications when there is misalignment between axes, Figure 6. Modified spur gears are commonly used to avoid the harmful edge effect.

The main direction of the modified spur gears is to replace the line contact by a point contact. This means to localize their bearing contact by a proper modification of the surface of one of the mating gears, the pinion being the preferred one.

5 Conclusions

A robust and very fast semi-analytical method, Non-Hertz, is presented to solve the concentrated contacts achieved between conjugate teeth during meshing.
An analytical method was developed to find the matrix of separations between the surfaces of the conjugate teeth.
The harmful edge effect has been pointed out and the need for flank modification and its analysis was revealed.

References

1. S. Li, Mechanism and Machine Theory, **42**, 6 (2007)
2. Y. Siang-Yu, T. Shyi-Jeng, Mechanism and Machine Theory, **97**, 190-214 (2016)
3. F. Sadeghi, B. Jalalahmadi, T. Slack, N. Raje, N. Arakere, ASME J. Tribol., **131**, 2 (2009)
4. K. Johnson, *Contact mechanics*, Cambridge University Press (1985)
5. F. Litvin, A. Fuentes, *Gear geometry and applied theory*, Cambridge University Press (2004)
6. ISO 6336-1, *Calculation of load capacity of spur and helical gears*, Switzerland (2006)
7. I. Polonsky, L. Keer, ASME J. Tribol. **122,** 1 (2000)
8. S. Creţu, E. Antalucă, O. Creţu, Annals Univ. Galaţi Romania **24**, 26-35 (2003)
9. S. Creţu, Bull. Inst.Polit. Iași, **LI (LV)** 1-2, 1-31 (2005)
10. S. Creţu, Elastic plastic concentrated contact (in Romanian), Ed. Politehnium, Iaşi, Romania (2009)
11. N. Pop, S. Creţu, A. Tufescu, App. Mech. Mat. **658**, 531-356 (2014)
12. STAS 821, Romania (1982)
13. R. Guibault, ASME J. Tribol. **133**, 2 (2011)
14. S. Creţu, M. Benchea, A. Iovan-Dragomir, J. Balkan Tribol. Assoc. **22**, 1 (2016)
15. N. Popinceanu, E. Diaconescu, S. Creţu, Wear, **71**, 265-282 (1981)